

The 3d magnetization at first-order transitions of the rare earth Laves phases  $R_{1-x}Y_xCo_2$  studied by measurements of magnetic hyperfine fields

This article has been downloaded from IOPscience. Please scroll down to see the full text article.

2006 J. Phys.: Condens. Matter 18 253

(<http://iopscience.iop.org/0953-8984/18/1/018>)

View [the table of contents for this issue](#), or go to the [journal homepage](#) for more

Download details:

IP Address: 129.252.86.83

The article was downloaded on 28/05/2010 at 07:59

Please note that [terms and conditions apply](#).

# The 3d magnetization at first-order transitions of the rare earth Laves phases $R_{1-x}Y_xCo_2$ studied by measurements of magnetic hyperfine fields

M Forker<sup>1</sup>, P de la Presa<sup>1,4</sup> and A F Pasquevich<sup>2,3</sup>

<sup>1</sup> Helmholtz-Institut für Strahlen- und Kernphysik der Universität Bonn, Nussallee 14-16, D-53115 Bonn, Germany

<sup>2</sup> Departamento de Física, Facultad de Ciencias Exactas, Universidad de La Plata, La Plata, Argentina

<sup>3</sup> Comisión de Investigaciones Científicas de la Provincia de Buenos Aires, Argentina

E-mail: [forker@iskp.uni-bonn.de](mailto:forker@iskp.uni-bonn.de)

Received 16 August 2005

Published 9 December 2005

Online at [stacks.iop.org/JPhysCM/18/253](http://stacks.iop.org/JPhysCM/18/253)

## Abstract

The magnetic phase transitions of pseudo-binary rare earth (R) Laves phases  $R_{1-x}Y_xCo_2$  have been investigated by perturbed angular correlation (PAC) measurements of the magnetic hyperfine fields at the probe nucleus  $^{111}Cd$  for  $R = Tb, Sm$  and  $Ho$  at various  $Y$  concentrations  $x$  and for  $R = Gd, Dy, Er, Nd$  and  $Pr$  at the concentration  $x = 0.3$ . First-order transitions were observed in  $Tb_{1-x}Y_xCo_2$  and  $Sm_{1-x}Y_xCo_2$  for  $x \geq 0.3$ , in  $Ho_{1-x}Y_xCo_2$  for  $x \leq 0.4$  and in  $R_{0.7}Y_{0.3}Co_2$  for  $R = Dy, Ho, Er, Nd$  and  $Pr$ . For  $Gd_{0.7}Y_{0.3}Co_2$ , the temperature dependence of the average magnetic hyperfine field is compatible with a second-order transition. The discontinuity of the magnetic hyperfine interaction at the first-order transitions of heavy  $R_{1-x}Y_xCo_2$ , which mainly reflects the jump of 3d magnetization of the Co subsystem at  $T_C$ , was found to increase monotonically with decreasing order temperature. The  $T_C$  dependence of the normalized magnetic frequency  $\nu_M(T_C)/\nu_M(0) \propto [1 - (T_C/T_0)^2]^{1/2}$  with  $T_0 = 203(5)$  K for the boundary temperature between first- and second-order transitions can be explained by the temperature dependence of the coefficient of the  $M^4$  term of the free energy in the Wohlfarth–Rhodes–Shimizu theory of itinerant electron metamagnetism.

## 1. Introduction

The metamagnetic transition [1] of the itinerant 3d-electron system of the C15 Laves phases  $RCo_2$  ( $R =$  rare earth) from a paramagnetic to a highly magnetized state is a subject of

<sup>4</sup> Present address: Instituto de Magnetismo Aplicado, PO Box 155, 28230 Las Rozas (Madrid), Spain.

longstanding interest [2, 3]. In the phenomenological Wohlfahrt and Rhodes theory of metamagnetism [1] the magnetic state of an itinerant d-electron system in a magnetic field  $\mathbf{B}$  is discussed in terms of a Landau expansion of the free energy in powers of the d magnetization  $M_d$

$$F(M_d) = \frac{1}{2}a_1(T)M_d^2 + \frac{1}{4}a_3(T)M_d^4 + \frac{1}{6}a_5(T)M_d^6 + \dots - M_d \cdot \mathbf{B}. \quad (1)$$

The expansion coefficients  $a_i(T)$  depend on the density of states  $N(E)$  and its derivatives near the Fermi energy  $E_F$  [4, 5]. Their temperature dependence comes from Stoner excitations and from spin fluctuations [6] at higher temperatures. In  $\text{RCO}_2$ , the field driving the metamagnetic transition is the molecular field  $B_{\text{mol}}$  representing the exchange interaction between the 3d and the 4f sublattice. In this case, the 4f magnetization has to be taken into account in the Landau expansion of the free energy [7].

Among the interesting magnetic properties of the  $\text{RCO}_2$  Laves phases is the fact that with decreasing order temperature  $T_C$  the transition from the para- to the ferromagnetic state changes—at  $T_C \sim 200$  K—from second to first order. The compounds with the constituents  $R = \text{Gd}, \text{Tb}$  and  $\text{Sm}$  ( $T_C = 392, 231$  and  $206$  K, respectively) exhibit second-order transitions (SOTs), those with  $R = \text{Dy}, \text{Ho}, \text{Er}, \text{Nd}$  and  $\text{Pr}$  ( $T_C = 138, 78, 34, 98$  and  $40$  K, respectively) first-order transitions (FOTs) [8].

This change from second to first order has been related by Bloch *et al* [4], Shimizu [5, 9] and Inoue and Shimizu [7, 10] to the sign of the  $M^4$  term in the Landau expansion. Metamagnetic first-order transitions in a paramagnetic compound ( $a_1 > 0, a_5 > 0$ ) require  $a_3 < 0$ , while  $a_3 > 0$  results in second-order transitions. It has been shown by Bloch *et al* [4] that the band structure of  $\text{YCo}_2$  leads to a temperature dependence of the  $a_3$ -coefficient of approximately

$$a_3(T) = a_3(0)[1 - (T/T_0)^2]; \quad a_3(0) < 0. \quad (2)$$

Assuming the same band structure for  $\text{RCO}_2$ ,  $T_0$  thus constitutes the boundary between first-order ( $T_C < T_0$ ) and second-order ( $T_C > T_0$ ) transitions in the  $\text{RCO}_2$  series. From the temperature dependence of the paramagnetic susceptibility of  $\text{YCo}_2$ , Bloch *et al* [4] estimated  $T_0 \sim 250$  K while Inoue and Shimizu [10] arrived—on the basis of the order in  $\text{DyCo}_2$  and  $\text{Gd}_{1-x}\text{Y}_x\text{Co}_2$ —at an SOT–FOT boundary temperature of  $T_0 \approx 150$  K.

The correlation between the order of the transition and the order temperature has been studied experimentally with a number of techniques by magnetically diluting a given compound of the  $\text{RCO}_2$  series with non-magnetic La, Y, Lu or a different 4f element  $R'$ , which allows a systematic variation of the order temperature [11–15].

In the present paper, we report dilution experiments of this type aiming mainly at the discontinuity of the 3d magnetization at the first-order transitions of  $\text{RCO}_2$  and its variation with  $T_C$ . Information on the 3d magnetization can be obtained by measurements of the magnetic hyperfine fields  $B_{\text{hf}}$  experienced by the nuclei of closed-shell probe atoms.

The magnetic hyperfine field at the nuclei of non-rare-earth atoms in magnetically ordered compounds is caused by the Fermi contact term in the nucleus–electron interaction and reflects the spin polarization of the s electrons at the probe nucleus. A finite s-electron spin density may arise from the spin polarization of the host conduction electrons, the polarization of the electron core of the probe by a localized spin and the overlap of the valence electrons of the probe with spin polarized valence electrons of the magnetic ions. In the case of probe nuclei with closed electronic shells, core polarization plays no role and the dominant source of  $B_{\text{hf}}$  is the s-electron spin polarization induced by the host moments.

In the 3d metals Fe, Co and Ni a finite s-electron spin density arises from the s–d hybridization of the wide s band mixed with a narrow spin-polarized d band [16]. In these elemental ferromagnets, the hyperfine field at a given closed-shell probe is in a good approximation proportional to the 3d moment. In the case of  $\text{RCO}_2$ , both the 3d and the

4f sublattice contribute to the s-electron spin density, with the dominant contribution coming from the spin-polarized 3d band [17]. It is justified to assume that—as in Fe, Co and Ni—the 3d contribution to  $B_{\text{hf}}$  of closed-shell probes in  $R\text{Co}_2$  is proportional to the Co moment. Measurements of the hyperfine field in  $(R, Y)\text{Co}_2$  are then a way to study the discontinuous splitting of the Co d band at the FOTs as a function of the order temperature.

In the experiments reported here, the magnetic hyperfine field at the closed-shell probe  $^{111}\text{Cd}$  on the R site of  $R_{1-x}Y_x\text{Co}_2$  has been investigated by perturbed angular correlation (PAC) measurements as a function of temperature and Y concentration for the R constituents  $R = \text{Tb}, \text{Sm}$  and  $\text{Ho}$ . The study concentrates on the constituents  $R = \text{Tb}$  and  $\text{Sm}$  because the Curie temperatures of the SOTs of  $\text{TbCo}_2$  and  $\text{SmCo}_2$  ( $T_C = 231.4$  and  $206.4$  K, respectively) are close to the borderline between second- and first-order transitions. As the decrease of  $T_C$  with increasing Y content  $x$  is approximately linear, relatively small Y concentrations should be sufficient to reduce the Curie temperatures of  $\text{Tb}_{1-x}\text{Y}_x\text{Co}_2$  and  $\text{Sm}_{1-x}\text{Y}_x\text{Co}_2$  below  $T_0 \sim 200$  K, so that for these compounds the first-order discontinuity of the 3d magnetization can be studied over a large range of order temperatures.

The concentration dependence of the phase boundary between first- and second-order transitions of  $R_{1-x}Y_x\text{Co}_2$  has been calculated by Inoue and Shimizu [10]. For  $R = \text{Er}$  and  $\text{Ho}$ , this calculation predicts a change from first to second order at  $x \sim 0.15$  and  $x \sim 0.4$ , respectively. In an attempt to observe this change-over by hyperfine field measurements, we have extended this PAC study to  $\text{Ho}_{1-x}\text{Y}_x\text{Co}_2$ ;  $0 \leq x \leq 0.6$ . Additional measurements of  $B_{\text{hf}}(T)$  were carried out in  $\text{R}_{0.7}\text{Y}_{0.3}\text{Co}_2$  for  $R = \text{Gd}, \text{Dy}, \text{Er}, \text{Nd}$  and  $\text{Pr}$ .

## 2. Experimental details

### 2.1. Sample preparation and equipment

The PAC measurements were carried out with the 171–245 keV cascade of  $^{111}\text{Cd}$ , which is populated by the electron capture decay of the 2.8 d isotope  $^{111}\text{In}$ . The samples were produced by arc melting of the metallic components in the stoichiometric ratio in an argon atmosphere and characterized by x-ray diffraction. Most of the heavy R compounds were single C15 phases. Although the samples were remelted several times for homogenization, a slight contamination by a foreign phase, possibly  $\text{YCo}_3$ , was observed in a few cases. The relative intensity of this foreign phase was usually  $\leq 5\%$ , except for  $\text{Sm}_{1-x}\text{Y}_x\text{Co}_2$ , where spurious phases sometimes amounted to 15%. The samples were doped with the PAC probe  $^{111}\text{In}/^{111}\text{Cd}$  by diffusion (800 °C, 12 h) of carrier-free  $^{111}\text{In}$  into the host lattices. The PAC measurements were carried out with a standard four-detector  $\text{BaF}_2$  set-up. A closed-cycle He refrigerator was used for the temperature variation between 10 and 300 K with a temperature stability of about 0.1 K.

### 2.2. Data analysis

The angular correlation theory of two successive  $\gamma$ -rays of a  $\gamma$ - $\gamma$  cascade, expressed by angular correlation coefficients  $A_{kk}$  ( $k = 2, 4$ ) may be modulated in time by hyperfine interactions in the intermediate state of the cascade. For polycrystalline samples this modulation can be described by the perturbation factor  $G_{kk}(t)$  which depends on the multipole order, the symmetry and time dependence of the interaction and the spin of the intermediate state (for details see e.g. [18]).

The absence of an electric quadrupole at  $^{111}\text{Cd}$  in paramagnetic  $R\text{Co}_2$  [17] shows that the probe atom resides on the cubic R site. In the ferromagnetic phase we are therefore dealing with a perturbation by pure magnetic interaction, characterized by the Larmor frequency

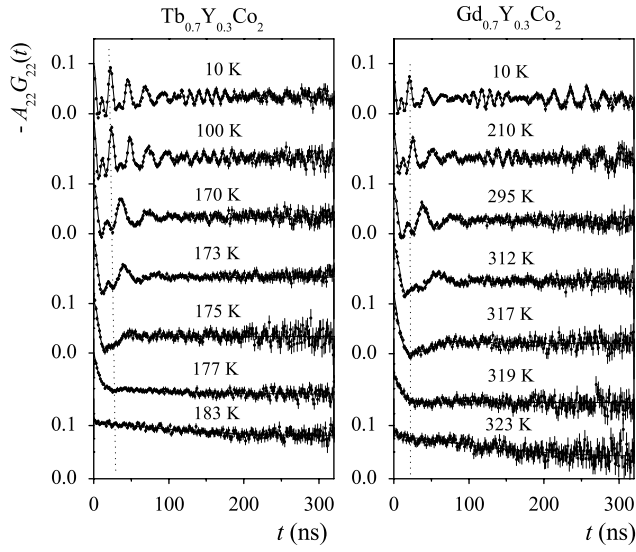


**Figure 1.** PAC spectra of  $^{111}\text{Cd}$  in  $\text{Tb}_{0.7}\text{Y}_{0.3}\text{Co}_2$  and  $\text{Gd}_{0.7}\text{Y}_{0.3}\text{Co}_2$  at different temperatures. The dotted vertical lines mark the precession period at 10 K.

$\omega_M = 2\pi\nu_M = g\mu_N B_{\text{hf}}/\hbar$  ( $\mu_N$  denotes the nuclear magneton,  $g$  the nuclear  $g$ -factor). In this case the perturbation factor can be expressed in analytical form:

$$G_{22}(t) = 1/5 + 2/5 \sum_{n=1,2} \cos(n\omega_M t) \exp(-\delta n\omega_M t). \quad (3)$$

The exponential factor accounts for a possible distribution of the magnetic hyperfine field. If the ensemble of probe nuclei is subject to a distribution rather than a unique hyperfine interaction, the nuclear spins of the ensemble no longer precess all with the same frequency and an attenuation of the oscillation amplitudes results, which is stronger for broader distributions. The parameter  $\delta$  is the relative width of a Lorentzian distribution.

Frequently, several fractions of nuclei subject to different hyperfine interactions are found in the same sample. In this case, the effective perturbation factor is given by

$$G_{kk}(t) = \sum_i f_i G_{kk}^i(t) \quad (4)$$

$f_i$  (with  $\sum_i f_i = 1$ ) is the relative intensity of the  $i$ th fraction.

### 3. Measurements and results

#### 3.1. $\text{Tb}_{1-x}\text{Y}_x\text{Co}_2$ and $\text{Sm}_{1-x}\text{Y}_x\text{Co}_2$

The temperature dependence of the magnetic hyperfine field of  $^{111}\text{Cd}$  was investigated in  $\text{Tb}_{1-x}\text{Y}_x\text{Co}_2$  in the concentration range  $0 \leq x \leq 0.7$ , in  $\text{Sm}_{1-x}\text{Y}_x\text{Co}_2$  at  $x = 0.3, 0.4$  and  $0.65$ . The two classes of PAC spectra observed in this study are illustrated in figures 1 and 2. Figure 1 shows spectra measured in  $\text{Tb}_{0.7}\text{Y}_{0.3}\text{Co}_2$  and  $\text{Gd}_{0.7}\text{Y}_{0.3}\text{Co}_2$ , figure 2 spectra observed in  $\text{Er}_{0.7}\text{Y}_{0.3}\text{Co}_2$  and  $\text{Sm}_{0.35}\text{Y}_{0.65}\text{Co}_2$ . In  $\text{Tb}_{0.7}\text{Y}_{0.3}\text{Co}_2$  and  $\text{Gd}_{0.7}\text{Y}_{0.3}\text{Co}_2$ , the precession period clearly increases towards higher temperatures. In  $\text{Er}_{0.7}\text{Y}_{0.3}\text{Co}_2$  and  $\text{Sm}_{0.35}\text{Y}_{0.65}\text{Co}_2$ , however, the precession period barely changes with temperature before the abrupt disappearance of the magnetic oscillation at the Curie temperature, which is a clear indication of a first-order transition.

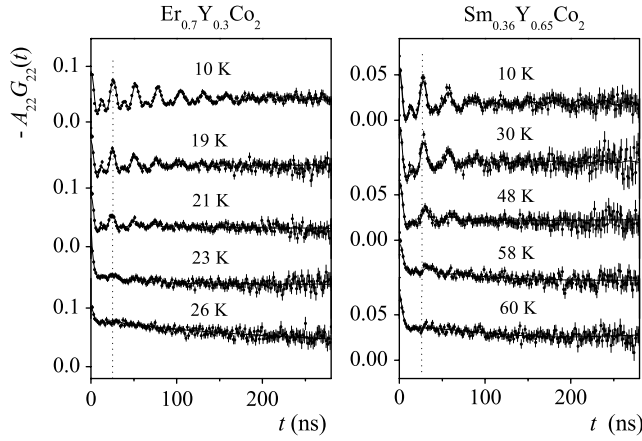


**Figure 2.** PAC spectra of  $^{111}\text{Cd}$  in  $\text{Er}_{0.7}\text{Y}_{0.3}\text{Co}_2$  and  $\text{Sm}_{0.35}\text{Y}_{0.65}\text{Co}_2$  at different temperatures. The vertical lines mark the precession period at 10 K.

At low temperatures and low Y concentrations of  $\text{Tb}_{1-x}\text{Y}_x\text{Co}_2$  and in  $\text{Gd}_{0.7}\text{Y}_{0.3}\text{Co}_2$  one observes a complex modulation pattern caused by the superposition of several components with different, well defined magnetic hyperfine frequencies  $\nu_M^i$  (see the 10 K spectra in figure 1). This superposition reflects the statistical occupation of the four nearest neighbour R sites of the  $^{111}\text{Cd}$  probe nucleus by non-magnetic Y. At temperatures  $T < 0.75 T_C$ , the difference in the frequencies  $\nu_M^i$  is sufficiently large to allow the separation of these components in the analysis. Their relative intensities  $f_i$  and frequencies  $\nu_M^i$  can be determined by fitting equations (3) and (4) to the experimental data. The details of the analysis of the low temperature spectra at 10 K are described elsewhere [19]. At  $T > 0.75 T_C$ , the frequency differences have for most concentrations decreased to the point where a reliable separation of the different components becomes difficult. For  $T > 0.75 T_C$ , the spectra of  $\text{Tb}_{1-x}\text{Y}_x\text{Co}_2$  and  $\text{Gd}_{0.7}\text{Y}_{0.3}\text{Co}_2$  were therefore analysed assuming a single site subject to a broad hyperfine field distribution. The parameters derived in this case are the average magnetic interaction frequency and the relative width  $\delta$  of the frequency distribution. The same procedure had to be applied to the spectra of  $\text{Sm}_{1-x}\text{Y}_x\text{Co}_2$  at all temperatures, because even at 10 K the frequencies  $\nu_M^i$  are too close to each other to be reliably separated.

Close to the Curie temperature  $T_C$ , the spectra of  $\text{Tb}_{1-x}\text{Y}_x\text{Co}_2$  with  $x \leq 0.7$  and those of  $\text{Gd}_{0.7}\text{Y}_{0.3}\text{Co}_2$  show two characteristic features: (i) the precession amplitudes are increasingly damped, and (ii) the evolution from the pattern of a magnetic perturbation towards the unperturbed anisotropy of the paramagnetic phase extends over a finite temperature interval  $\Delta T$ . As discussed in detail in [8], these observations are evidence for a finite distribution of the magnetic order temperature which leads to the coexistence of the ferro- and the paramagnetic phase and the divergence of the relative line width of the magnetic frequency in a small interval  $\Delta T$  around  $T_C$ . The spectra close to  $T_C$  were therefore analysed assuming two fractions of PAC probes, one with relative intensity  $f_{\text{paramag}}$  describing probes in the paramagnetic phase, the other one with intensity  $(1 - f_{\text{paramag}})$  describing probes in the ferromagnetic phase. In the ferromagnetic phase the perturbation factor is given by (3), in the paramagnetic phase one has  $G_{22}^{\text{paramag}}(t) \approx 1$ . Figure 3 illustrates the typical temperature dependence of the paramagnetic fraction and of the relative line width  $\delta$  observed close to the magnetic phase transitions of  $\text{Tb}_{1-x}\text{Y}_x\text{Co}_2$ . The data shown in figure 3 were extracted from the spectra of  $\text{Tb}_{0.7}\text{Y}_{0.3}\text{Co}_2$  in figure 1.

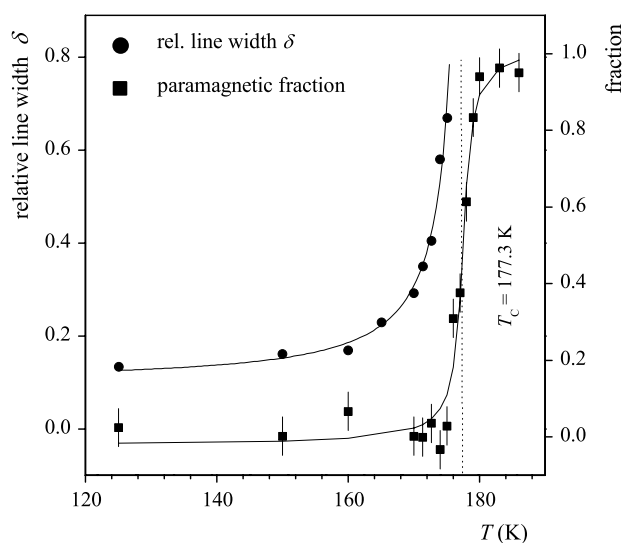


**Figure 3.** The relative line width  $\delta$  and the paramagnetic fraction  $f$  close to the magnetic phase transition of  $\text{Tb}_{0.7}\text{Y}_{0.3}\text{Co}_2$ .

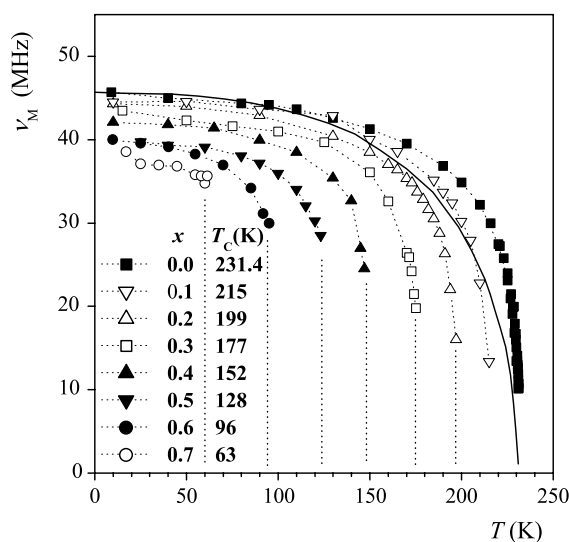


**Figure 4.** Temperature dependence of the site-averaged magnetic interaction frequency  $\nu_M$  of  $^{111}\text{Cd}$  in  $\text{Tb}_{1-x}\text{Y}_x\text{Co}_2$  at Y concentrations  $0 \leq x \leq 0.7$ . The solid line corresponds to the magnetization in the Stoner theory of itinerant electron ferromagnetism, normalized to  $\nu_M(T)$  of  $\text{TbCo}_2$ .

Figures 4 and 5 show the site-averaged interaction frequencies of  $^{111}\text{Cd}$  in  $\text{Tb}_{1-x}\text{Y}_x\text{Co}_2$ ,  $x \leq 0.7$ , and  $^{111}\text{Cd}$  in  $\text{Sm}_{1-x}\text{Y}_x\text{Co}_2$ ,  $x \leq 0.65$ , as a function of temperature for the different Y concentrations. Figure 5 also contains the frequencies of  $^{111}\text{Cd}$  in  $\text{Gd}_{1-x}\text{Y}_x\text{Co}_2$ ,  $x = 0.0, 0.3$ . All values for  $x = 0.0$  are taken from [8]. In most cases the frequencies were determined by adjusting the centre frequency and the line width of a single-site Lorentzian frequency distribution to the measured spectra. For those temperatures and  $x$ -values of  $\text{Tb}_{1-x}\text{Y}_x\text{Co}_2$  for which the different magnetic components could be separated without the constraint of fixed

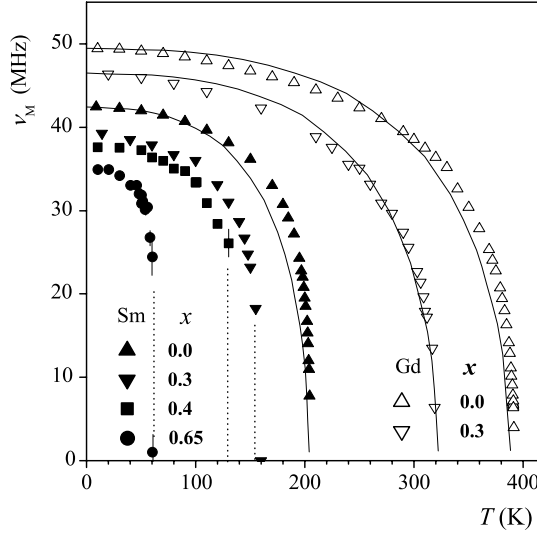


**Figure 5.** Temperature dependence of the site-averaged magnetic interaction frequency  $\nu_M$  of  $^{111}\text{Cd}$  in  $\text{Sm}_{1-x}\text{Y}_x\text{Co}_2$  (full symbols) at the Y concentrations  $x = 0.0, 0.3, 0.4$  and  $0.65$  ( $T_C = 206, 157, 130,$  and  $70$  K, respectively) and in  $\text{Gd}_{1-x}\text{Y}_x\text{Co}_2$  (open symbols) at  $x = 0.0$  and  $0.3$  ( $T_C = 392$  and  $323$  K, respectively). The solid lines correspond to the magnetization in the Stoner theory of itinerant electron ferromagnetism.

Lorentzian width, the site-averaged frequency  $\nu_M(T) = \sum_{i=1}^4 f_i \nu_M^i(T)$  is shown. The smallest frequency displayed in figures 4 and 5 for a given combination of R and  $x$  corresponds to the highest temperature at which the spin precession has some still visible amplitude (e.g.  $T = 175$  and  $317$  K for  $\text{Tb}_{0.7}\text{Y}_{0.3}\text{Co}_2$  and  $\text{Gd}_{0.7}\text{Y}_{0.3}\text{Co}_2$ , respectively (figure 1) and  $T = 23$  and  $58$  K for  $\text{Er}_{0.7}\text{Y}_{0.3}\text{Co}_2$  and  $\text{Sm}_{0.35}\text{Y}_{0.65}\text{Co}_2$ , respectively (figure 2)). The Curie temperatures deduced from the  $\nu_M(T)$ -data of  $\text{Tb}_{1-x}\text{Y}_x\text{Co}_2$  are included in figure 4. The  $T_C$ -values of  $\text{Sm}_{1-x}\text{Y}_x\text{Co}_2$  are  $206, 157, 130,$  and  $70$  K at  $x = 0.0, 0.3, 0.4$  and  $0.65$ , respectively.

### 3.2. $R_{0.7}Y_{0.3}Co_2$ , $R = Gd, Dy, Er, Nd, Pr$

The PAC spectra of  $^{111}\text{Cd}$  in  $\text{Gd}_{0.7}\text{Y}_{0.3}\text{Co}_2$  show a pronounced similarity to those of  $\text{Tb}_{1-x}\text{Y}_x\text{Co}_2$  with  $x \leq 0.3$  (see figure 1). In particular, in both compounds one finds the same strong damping of the oscillation amplitudes and the coexistence of the para- and the ferromagnetic phase close to  $T_C$ . From the temperature dependence of the magnetic interaction frequencies of  $\text{Gd}_{0.7}\text{Y}_{0.3}\text{Co}_2$  one obtains an order temperature  $T_C = 321.0(1.5)$  K. In all other  $R_{0.7}\text{Y}_{0.3}\text{Co}_2$ , the transitions are clearly of first order with Curie temperatures of  $T_C = 96.5(5), 23(1), 71.0(5)$  and  $34(5)$  K for  $R = Dy, Er, Nd$  and  $Pr$ , respectively. As an example, figure 2 shows the spectra of  $\text{Er}_{0.7}\text{Y}_{0.3}\text{Co}_2$ . As reflected by the continuous decrease of the amplitude of the magnetic oscillation at  $T > 20$  K, the ferro- and the paramagnetic fractions coexist from  $\sim 20$  to  $\sim 26$  K. Nevertheless, the phase transition can be identified as of first order because the magnetic frequency practically does not change with temperature before the total disappearance of the magnetic oscillation.

### 3.3. $Ho_{1-x}Y_xCo_2$ ; $0 \leq x \leq 0.6$

The PAC of  $^{111}\text{Cd}$  in  $\text{Ho}_{1-x}\text{Y}_x\text{Co}_2$  was studied for the Y concentrations  $0 \leq x \leq 0.6$ . In the range  $0 \leq x \leq 0.4$ , the magnetic hyperfine field varied only very slightly with temperature and



disappeared—as in undiluted  $\text{HoCo}_2$  [8]—discontinuously at  $T_C$ , which are the characteristic features of an FOT. At  $x = 0.5$ , a broad quadrupole distribution appeared in the paramagnetic phase. Attempts to extract the magnetic hyperfine field from the resulting combined interaction in the ferromagnetic phase were unsuccessful. The changes in the PAC pattern allowed, however, an estimate of the Curie temperature:  $T_C \sim 30(5)$  K. For  $\text{Ho}_{0.4}\text{Y}_{0.6}\text{Co}_2$ , the PAC data suggest  $T_C < 15$  K.

## 4. Discussion

### 4.1. The order of the magnetic phase transitions of $\text{R}_{1-x}\text{Y}_x\text{Co}_2$

The magnetic phase transitions of the elemental ferromagnets Fe, Co, Ni and Gd have been investigated in great detail by measurements of the magnetic hyperfine interaction of suitable probe nuclei. In favourable cases, the hyperfine frequencies in the ferromagnetic phase have been determined down to reduced temperatures of  $(1 - T/T_C) \leq 10^{-4}$  [20]. In magnetically ordered intermetallics, however, the temperature range for precise frequency measurements appears to be limited to reduced temperatures of the order of  $(1 - T/T_C) \geq 10^{-2}$ . The reason for this limitation is the observation of a finite distribution of the order temperature in practically all intermetallic compounds investigated by hyperfine field measurements. The width  $\Gamma_C$  of this distribution is usually of the order of a few kelvin. As discussed in detail in [8], a  $T_C$ -distribution, which reflects a spatial variation of the exchange interaction possibly related to some site disorder in intermetallic compounds, leads to the divergence of the relative line width of the magnetic frequency and the coexistence of the ferro- and the paramagnetic phase in the interval  $\Delta T \approx \Gamma_C$  around  $T_C$  (note:  $\Delta T$  is at least one order of magnitude larger than the experimental distribution of the sample temperature). As a consequence, a precise determination of the frequency at reduced temperatures  $(1 - T/T_C) \leq \Gamma_C/T_C$  becomes difficult.

The effect of the  $T_C$ -distribution on the oscillation amplitudes is stronger the more the frequency at a given temperature  $T$  varies with the Curie temperature. Close to the  $T_C$  of an SOT,  $\nu_M$  decreases critically with decreasing  $T_C$ :  $\nu_M(T) = \nu_M(0)(1 - T/T_C)^\beta$  with an exponent of the order  $\beta \sim 0.3\text{--}0.4$  [20]. At  $T \approx T_C$ , small variations of the Curie temperature therefore produce broad distributions of  $\nu_M$ , while at low  $T$  the magnetic frequencies remain sharply defined. Such broad frequency distributions are found in the spectra of  $\text{Tb}_{0.7}\text{Y}_{0.3}\text{Co}_2$  and  $\text{Gd}_{0.7}\text{Y}_{0.3}\text{Co}_2$  (figure 1). At first-order transitions, the  $T_C$ -distribution is less damaging to the PAC oscillations because the variation of  $\nu_M$  with  $T_C$  is less pronounced. A distribution of the order temperature therefore produces a slighter variation of  $\nu_M$  and the resulting frequency distribution is narrower, even at  $T \approx T_C$ . The spectra of  $\text{Er}_{0.7}\text{Y}_{0.3}\text{Co}_2$  and  $\text{Sm}_{0.35}\text{Y}_{0.65}\text{Co}_2$  in figure 2 are examples for this situation: as the frequency varies only slightly with temperature, the magnetic oscillations remain clearly visible up to the complete disappearance of the ferromagnetic fraction.

The extraction of the relative width  $\Gamma_C$  of the  $T_C$ -distribution from  $f_{\text{param}}(T)$  and  $\delta(T)$  is discussed in [8]. Assuming a Lorentzian  $T_C$ -distribution, the temperature dependence of the paramagnetic fraction of  $\text{Tb}_{0.7}\text{Y}_{0.3}\text{Co}_2$  (solid line in figure 3) corresponds to a line width of  $\Gamma_C \approx 2.2$  K which is comparable to the values of  $\Gamma_C$  reported for non-diluted  $\text{RCO}_2$  [8]. The divergence of the relative line width  $\delta$  leads to  $\Gamma_C$ -values of the same order of magnitude. Similar values of  $\Gamma_C \approx 2\text{--}3$  K, corresponding to a ratio  $\Gamma_C/T_C \approx 10^{-2}$ , have been deduced from the paramagnetic fraction in the  $\text{R}_{1-x}\text{Y}_x\text{Co}_2$  compounds of the present study up to Y concentrations of  $x \leq 0.6$ . At concentrations  $x > 0.6$ , the width of the  $T_C$ -distribution was found to increase to  $\Gamma_C \leq 7$  K.

The  $T_C$ -distribution obstructs the identification of the order of the phase transition to some extent. With  $\Gamma_C/T_C \approx 10^{-2}$ , the lowest frequency (normalized to the low temperature

saturation value) to which an SOT can be reliably followed is of the order  $\nu_M(T)/\nu_M(0) \approx (\Gamma_C/T_C)^B \approx 0.2$ . Consequently, an FOT with a discontinuity of the frequency at  $T_C$  of  $\nu_M(T_C)/\nu_M(0) \leq 0.2$  cannot be distinguished from an SOT. This situation occurs in  $Tb_{1-x}Y_xCo_2$  at  $x = 0$  and  $0.1$  and to a lesser extent in  $Gd_{0.7}Y_{0.3}Co_2$  (see figures 4 and 5). In these cases, the frequency of the slowest spin precession with some still visible amplitude is close to the limit  $\nu_M(T_C)/\nu_M(0) \approx 0.2$  and a reliable determination of the order of the phase transition from  $\nu_M(T)$  becomes difficult. Even for  $TbCo_2$ , usually considered an SOT compound, an FOT with a small discontinuity of the order parameter would be compatible with our data.

For  $Tb_{1-x}Y_xCo_2$  with  $x \geq 0.3$ , however, the relative frequency jump at  $T_C$  is  $\nu_M(T_C)/\nu_M(0) \geq 0.3$  and the phase transitions can be safely classified as FOTs, which is in agreement with the conclusions of Duc *et al* [12] based on measurements of magnetization, electrical resistivity and specific heat. As in  $Tb_{1-x}Y_xCo_2$  with  $x \geq 0.3$ , the transitions in  $Sm_{1-x}Y_xCo_2$  with  $x = 0.3, 0.4$  and  $0.65$  are unquestionably of first order (see figure 5).

For  $Er_{0.7}Y_{0.3}Co_2$ , the temperature dependence of the  $^{111}Cd$  hyperfine interaction clearly reflects an FOT (see figure 2). In the same compound Duc *et al* [11] have observed a slow change of the magnetization around  $T_C$ , which these authors attribute to an SOT. A finite distribution of the order temperature, which we have found in all intermetallic compounds, would, however, also produce a similar behaviour of the magnetization for FOTs. In all other  $R_{1-x}Y_xCo_2$  investigated here, the magnetic phase transitions are of first order.

The concentration dependence of the Curie temperatures of  $R_{1-x}Y_xCo_2$  and their variation with the R constituent deduced from the present  $\nu_M(T)$ -data agree well with the values previously obtained for R = Gd [21, 22], Tb [12, 23, 24] and Ho [25]. A detailed discussion of these trends and their relation to the temperature dependence of the 3d susceptibility has been given by Duc *et al* [11, 12].

#### 4.2. The discontinuity of the magnetic hyperfine interaction of $^{111}Cd$ at first-order transitions of $R_{1-x}Y_xCo_2$

We express the discontinuity of the magnetic hyperfine interaction of  $^{111}Cd$  at the first-order transitions of  $R_{1-x}Y_xCo_2$  by the ratio  $\nu_M(T_C)/\nu_M(0)$ . The values of this ratio, extracted from the experimental  $\nu_M(T)$ -curves, are plotted in figure 6 versus the respective order temperature  $T_C$ .

For the heavy R = Tb, Dy, Ho, and Er, all values of  $\nu_M(T_C)/\nu_M(0)$  follow roughly the same trend: the relative frequency jump increases continuously with decreasing  $T_C$ , independent of the R constituent. The light R = Pr and Nd—including the undiluted  $RCo_2$ —show a similar variation. The absolute values of  $\nu_M(T_C)/\nu_M(0)$ , however, are smaller than in the heavy  $R_{1-x}Y_xCo_2$  at comparable order temperatures. The frequency discontinuities of  $Sm_{1-x}Y_xCo_2$  follow the trend of the heavy  $R_{1-x}Y_xCo_2$ .

For the interpretation of the  $T_C$ -dependence of the frequency jump in figure 6, it is important to stress that the dominant contribution to the hyperfine field of  $^{111}Cd$  in  $RCo_2$  comes from the Co 3d magnetization. This conclusion is based on the comparison of the hyperfine fields of  $^{111}Cd$  in isomorphous  $RCo_2$  and  $RNi_2$ . In the latter compound, there is practically no 3d magnetic moment. The magnetic order in  $RNi_2$  is sustained by indirect 4f–4f coupling alone and the  $^{111}Cd$  hyperfine field can therefore be taken as a measure of the 4f contribution to the electron spin polarization. For R = Tb, e.g., one has  $B_{hf}(TbCo_2) = 19.5$  T [17] and  $B_{hf}(TbNi_2) = 3.1$  T [26]. As the 3d and 4f contributions to  $B_{hf}(RCo_2)$  have the same relative sign [19], these data mean that the 4f contribution is about 15% of the 3d contribution and even less for R constituents with smaller 4f spin. The discontinuity of the frequency therefore reflects

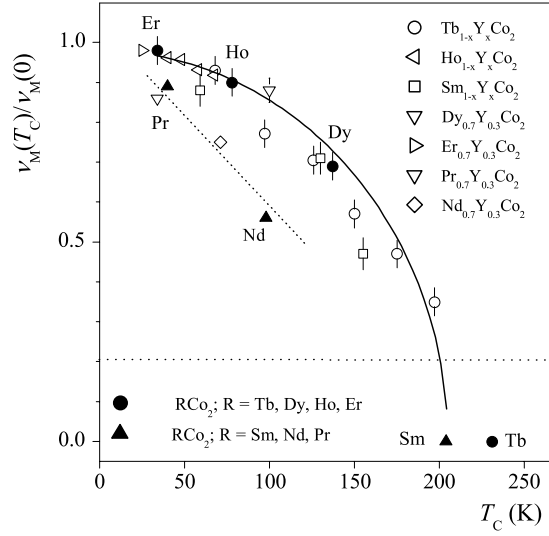


**Figure 6.** The discontinuous jump of the magnetic hyperfine frequency  $\nu_M(T_C)$  at the magnetic phase transition of  $R_{1-x}Y_xCo_2$ , normalized to the respective saturation value  $\nu_M(0)$ , as a function of the order temperature. The solid line represents a fit of the relation  $\nu_M(T_C) = \nu_M(0)[1 - (T/T_0)^2]^{1/2}$  to the experimental data. Because of the critical line broadening close to the phase transition, only frequencies  $\nu_M(T_C)/\nu_M(0) \geq 0.2$  can be determined accurately. This frequency limit is marked by the dashed horizontal line.

in a good approximation the jump of the Co 3d magnetization at the first-order transitions of  $R_{1-x}Y_xCo_2$ , and the variation of  $\nu_M(T_C)/\nu_M(0)$  in figure 6 then implies that the Co 3d moment induced at  $T_C$  by the 4f molecular field increases with decreasing order temperature.

A first-order transition requires that the free energy has two minima, separated by a maximum, one at  $M = 0$ , the other one at  $M = M_0 \neq 0$ . Such a situation is given when  $a_1(T_C) > 0$ ,  $a_3(T_C) < 0$  and  $a_5(T_C) > 0$  (see equations (1) and (2)). The corresponding magnetization curve  $M_d = f(H; a_i(T))$ , which can be deduced from  $H(M) = dF/dM$ , is S shaped and a first-order transition to the highly magnetized state occurs at some critical field  $H_C \neq 0$  if the quantity  $\frac{a_1 a_5}{a_3^2}$  is in the range  $\frac{9}{20} > \frac{a_1 a_5}{a_3^2} > \frac{3}{16}$ . In  $RCo_2$  the transition is driven by the 3d–4f exchange interaction and occurs—as explained by Cyrot and Lavagna [27]—at the temperature where the two equations describing the mutual dependence of the Co and R magnetizations  $M_d$  and  $M_R$  at different temperatures have a self-consistent solution.

The d-band magnetization at the critical field in the highly magnetized state has been expressed by Shimizu [9] in terms of the Landau coefficients  $a_i$ :

$$M_C^2 = -\frac{3a_3}{10a_5} \left[ 1 + \sqrt{1 - \frac{20}{9} \frac{a_1 a_5}{a_3^2}} \right]. \quad (5)$$

If one accepts that the hyperfine field is proportional to the Co magnetization, equation (5) relates the temperature dependence of the frequency jump  $\nu_M(T_C)/\nu_M(0)$  in figure 6 to the temperature dependence of the Landau coefficients. The coefficient  $a_5$  is usually considered to be constant [4]. Assuming that for  $RCo_2$  the coefficient  $a_1$  has the same temperature dependence as the inverse susceptibility of  $YCo_2$  [3] and that of  $a_3$  can be described by the Bloch relation (equation (2)), the variations of  $a_1$  and  $a_3^2$  in the square root term of equation (5) practically cancel. Under these conditions, the temperature dependence of the magnetization jump at the FOTs in  $RCo_2$  is mainly determined by that of the  $a_3$ -coefficient. Assuming that

$a_1a_5/a_3^2$  does not vary with temperature, one obtains from (5)

$$M'_C \propto C[1 - (T/T_0)^2]^{1/2}. \quad (6)$$

The solid line in figure 6 is the result of a fit of equation (6) to the experimental values of  $\nu_M(T_C)/\nu_M(0)$  of the heavy  $R_{1-x}Y_xCo_2$  and  $Sm_{1-x}Y_xCo_2$ . The experimental trend is well reproduced by the Wohlfarth–Rhodes–Shimizu theory of itinerant-electron metamagnetism. The fit leads to a boundary temperature between SOTs and FOTs of  $T_0 = 203(5)$  K. The differences between heavy  $R_{1-x}Y_xCo_2$  and  $Sm_{1-x}Y_xCo_2$  on the one hand and  $R_{1-x}Y_xCo_2$  with  $R = Nd$  and  $Pr$  on the other hand suggest a smaller magnitude of  $a_3(0)$  for these light R constituents.

## 5. Summary

We have studied properties of the magnetic phase transitions of  $R_{1-x}Y_xCo_2$  by PAC measurements of the magnetic hyperfine field  $B_{hf}$  of the probe nucleus  $^{111}Cd$  on the cubic R site of these C15 Laves phases. The magnetic hyperfine frequency, which is roughly proportional to the magnetic moment of the itinerant 3d electrons, was determined as a function of temperature for different Y concentrations and R constituents. In  $Tb_{1-x}Y_xCo_2$  and  $Sm_{1-x}Y_xCo_2$  the phase transitions are of first order for Y concentrations  $x \geq 0.3$ . For smaller concentrations, the temperature dependence of the magnetic hyperfine interaction is compatible with second-order transitions. First-order transitions were observed for all concentrations  $x \leq 0.4$  of  $Ho_{1-x}Y_xCo_2$  and in  $R_{0.7}Y_{0.3}Co_2$  with  $R = Dy, Er, Nd$ , and  $Pr$ .

The discontinuity of the magnetic hyperfine interaction at the first-order transitions of the heavy  $R_{1-x}Y_xCo_2$ , which mainly reflects the jump of 3d magnetization of the Co subsystem at  $T_C$ , was found to increase continuously with decreasing order temperature. The temperature dependence of the frequency jump  $\nu_M(T_C)/\nu_M(0) \propto [(1 - T/T_0)^2]^{1/2}$  with  $T_0 = 203(5)$  K for the boundary temperature between first- and second-order transitions can be related to that of the  $a_3$ -coefficient of the Landau expansion of the free energy.

## Acknowledgments

One of the authors (AFP) acknowledges financial support from AvH Foundation (Germany) and CICPBA (Argentina).

## References

- [1] Wohlfahrt E P and Rhodes P 1962 *Phil. Mag.* **7** 1818
- [2] Duc N H and Brommer P E 1999 *Handbook of Magnetic Materials* vol 12, ed K H J Buschow (Amsterdam: Elsevier Science) p 259
- [3] Gratz E and Markosyan A S 2001 *J. Phys.: Condens. Matter* **13** R385
- [4] Bloch D, Edwards M, Shimizu M and Voiron J 1975 *J. Phys. F: Met. Phys.* **5** 1217
- [5] Shimizu M 1981 *Rep. Prog. Phys.* **44** 329
- [6] Yamada H 1993 *Phys. Rev. B* **47** 11211
- [7] Inoue J and Shimizu M 1982 *J. Phys. F: Met. Phys.* **12** 1811
- [8] Forker M, Müller S, de la Presa P and Pasquevich A F 2003 *Phys. Rev. B* **68** 14409
- [9] Shimizu M 1982 *J. Physique* **43** 155
- [10] Inoue J and Shimizu M 1988 *J. Phys. F: Met. Phys.* **18** 2487
- [11] Duc N H, Hien T D, Brommer P E and Franse J J M 1988 *Physica B* **149** 352
- [12] Duc N H, Hien T D, Mai P P, Ngan N H K, Sinh N H, Brommer P E and Franse J J M 1989 *Physica B* **160** 199
- [13] Duc N H, Brommer P E and Franse J J M 1993 *Physica B* **191** 239
- [14] Garcia F, Soarez M R, Takeuchi A Y and da Cunha S F 1998 *J. Alloys Compounds* **279** 117

- 
- [15] Ouyang Z W, Rao G H, Yang H F, Liu W F, Liu G Y, Feng X M and Liang J K 2003 *Physica B* **334** 118
  - [16] Stearns M B 1973 *Phys. Rev. B* **8** 4383
  - [17] de la Presa P, Müller S, Pasquevich A F and Forker M 2000 *J. Phys.: Condens. Matter* **12** 3423
  - [18] Frauenfelder H and Steffen R M 1963 *Perturbed Angular Correlations* ed K Karlsson, E Matthias and K Siegbahn (Amsterdam: North-Holland)
  - [19] de la Presa P, Pasquevich A F and Forker M 2005 *Phys. Rev. B* **72** 134402
  - [20] Hohenemser C, Rosov N and Kleinhammes A 1989 *Hyperfine Interact.* **49** 267
  - [21] Tsuchida T, Sugaki S and Nakamura Y 1975 *J. Phys. Soc. Japan* **30** 340
  - [22] Baranov N V, Yermakov A A and Podlesnyak A 2003 *J. Phys.: Condens. Matter* **15** 5371
  - [23] Berthier Y, Gignoux D and Tari A 1986 *J. Magn. Magn. Mater.* **58** 265
  - [24] Pasquevich A F, Fernández van Raap B, Forker M and de la Presa P 2004 *Physica B* **354** 357
  - [25] Steiner W, Gratz E, Ortbauer H and Camen H W 1978 *J. Phys. F: Met. Phys.* **8** 1525
  - [26] Forker M, de la Presa P, Müller S, Lindbaum A and Gratz E 2004 *Phys. Rev. B* **70** 14302
  - [27] Cyrot M and Lavagna M 1979 *J. Physique* **40** 763